MODELING AND ANALYSIS OF POOLED STEPPED CHUTES

Graziano Guerra

Dipartimento di Matematica e Applicazioni
Università degli studi di Milano–Bicocca
Via Roberto Cozzi, 53 - 20125 Milano, Italy

Michael Herty

Mathematik (Kontinuierliche Optimierung)
RWTH Aachen University
Templergraben 55 D-52056 Aachen, Germany

Francesca Marcellini

Dipartimento di Matematica e Applicazioni
Università degli studi di Milano–Bicocca
Via Roberto Cozzi, 53 - 20125 Milano, Italy

(Communicated by Axel Klar)

Abstract. We consider a mathematical model describing pooled stepped chutes where the transport in each pooled step is described by the shallow–water equations. Such systems can be found for example at large dams in order to release overflowing water. We analyze the mathematical conditions coupling the flows between different chutes taken from the engineering literature. For the case of two canals divided by a weir, we present the solution to the Riemann problem for any initial data in the subcritical region, moreover we give a well–posedness result. We finally report on some numerical experiments.

1. **Introduction.** This work deals with the modelling of water flow in the so called pooled stepped chutes. This geometry is frequently found in dams and it also appears in mountain rivers to control the bed load transport. In both cases the main concern is to spill excessive floodwater in additional channels next to the dam structure. These are called pooled stepped chutes or pooled steps. Within the pooled steps additional weirs perpendicular to the flow direction are introduced to increase energy dissipation. This problem has gained some attention in recent years in the engineering community, see e.g. [5, 7, 8, 9, 10, 25, 28, 30]. However, only a few mathematical discussions are currently available [18, 27]. In particular, the modeling and design of the spillways and stepped channels have so far been addressed using experiments and data fitting techniques, see e.g. [30]. From the measurements empirical formulas have been derived and used in sophisticated simulations. Empirical formulas and tables of overflow velocities and water heights over a weir can be found for example in [19].

So far, the mathematical discussion has been limited to a consideration of the effect of the weir at the end of a spillway *neglecting* the dynamics of the water inside the pooled channels. Here, we discuss the mathematical implications of considering

the coupled problem, i.e., the dynamics inside the pooled steps and the (empirical or theoretical) conditions imposed closed to the weir. Typically, the water flow in the channels is described by the shallow–water equations whereas the effect of the weir is given by some algebraic conditions. We treat this problem using a network approach with the conditions at the weir as coupling conditions. We present a well–posedness result for a simple condition based on energy dissipation. The recent literature offers several results on the modeling of systems governed by conservation laws on networks. For instance, in [1, 2, 11, 14] the modeling of a network of gas pipelines is considered. The basic model is the p-system or, in [15, 20], the full set of Euler equations. The key problem in these papers is the description of the evolution of fluid at a junction between two or more pipes. A different physical problem, leading to a similar analytical framework, is that of the flow of water in open channels. The recent literature on water flow in open canals where similar analytical problems appear is very rich and we only refer to a few publications in this direction [22, 17, 24, 23]. In these works the governing equations are as below the St. Venant equations and they are coupled at nodes in order to describe water flow in connected domains. A variety of coupling conditions exist and have been discussed depending on whether the node is controllable by a gate or not. In the case of gates controllability and stabilization properties have been established [17, 24, 3]. Those conditions are applicable in the case of waterways or small rivers. Note that here we have different setting in mind. We consider the problem on a different length scale. Our scale is smaller since we are only interested in the overspill water flow next to a dam. Therefore, we need to include the small weir in the model which influences the water dynamics. We furthermore do not have any control measures. The analysis of the problem is therefore closely related to the work of [1, 11] and we can consider weak solutions. The presented results in [16, 21, 22, 17]are based on solutions of higher regularity used in particular for control measures.

Consider a water flow in an open canal affected by a weir or small dam at the point $x = 0$. If the water level becomes greater than the height of the weir, some water passes over the weir. Similarly to the models in [16, 21, 22, 17] we describe the dynamics of the water by the shallow water equations, while the interaction with the weir is described by coupling conditions.

Let $(h, v)(t, x)$ be respectively the water level (with respect to the flat bottom) and its velocity for $x \neq 0$. The shallow–water equations in each canal are given by

$$\begin{cases} \partial_t h + \partial_x (hv) = 0 \\ \partial_t (hv) + \partial_x \left(hv^2 + \frac{1}{2} gh^2 \right) = 0 \end{cases} \qquad x \neq 0, \tag{1}$$

where g is the gravity constant. Two canals are coupled by so–called pooled steps [30]. A sketch of this situation is given in Figure 1. In the engineering literature [10, 29, 30] (see also Remark 1) water of height h^- flowing over a weir of height H^- generates a flow Q

$$Q = C \left(h^- - H^- \right)^{3/2}, \text{ with } C = \tilde{C} \sqrt{g}, \tag{2}$$

where $\tilde{C} \leq 1$ is a constant depending on the air–water–ratio and the detailed geometry. In many situations $\tilde{C} = 0.6$ is used. The equation (2) is called $3/2$−law. Formally, it can be derived from the following idea: the potential energy of the water flowing over the weir is transformed to kinetic energy. Indeed, if ρ is the water density, a water column of height $h = h^- - H^-$ and mass (per unit area) ρh at rest over a step is provided with a potential energy per unit surface equal to $(\rho h) \frac{1}{2} gh$.
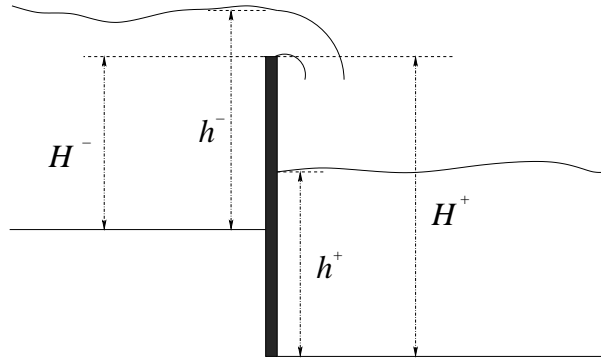
FIGURE 1. This figure represents two connected pooled steps with a weir in between and the indication of the various heights

If all the potential energy of the water mass (per unit surface) ρh becomes kinetic energy when it falls down the weir at $h = 0$ we have the balance

$$(\rho h)\frac{1}{2}gh = \frac{1}{2}(\rho h)v^2.$$

Solving for v in terms of h we obtain the previous formula and $1 - \tilde{C}$ is the percentage of energy loss during the change of potential to kinetic energy. We use this idea to deduce the coupling condition for (1) at $x = 0$. We conserve the total water over the weir and hence $h^+ v^+ = h^- v^-$. The difference in the amount of water overflowing the weir is $[h^- - H^-]_+ - [h^+ - H^+]_+$. This defines the velocity (and its sign) at the weir according to the balance of potential and kinetic energy. Hence, the coupling conditions are

$$\begin{cases} h^- v^- = C\left([h^- - H^-]_+ - [h^+ - H^+]_+\right) \cdot \sqrt{\left|[h^- - H^-]_+ - [h^+ - H^+]_+\right|} \\ h^+ v^+ = h^- v^-, \end{cases} \tag{3}$$

where $C = 0.6\sqrt{g}$, $(h^-, v^-) = (h, v)(t, 0-)$, $(h^+, v^+) = (h, v)(t, 0+)$ while $H^\pm$ are the heights of the weir to the left and the right (see Figure 1).

Remark 1. Obviously, (2) is only a first approximation on the complex dynamics at the weir, see [8, 27, 30]. As outlined in the introduction there exists a variety of empirical formulas in the engineering community. Many of them include further effects as for example the water–air ratio of the overspill or the roughness of the channel bottom. For example in [30, Equation 7.7] the following relation has been determined

$$Q = \left(h^- - H^-\right)^{3/2}\left(\frac{2}{3}\mu\sqrt{2g}\right) =$$

$$C_1\sqrt{g}\left(h^- - H^-\right)^{3/2} + C_2\sqrt{g}\left(h^- - H^-\right)^{5/2}/H^-.$$

Here, we have $\mu = 0.611 + 0.08(h^- - H^-)/H^-$ and the constants are $C_1 = \frac{2}{3}\sqrt{2}\,0.611$ and $C_2 = \frac{2}{3}\sqrt{2}\,0.08$. Since the coefficient C_1 is roughly eight times larger than C_2, this equation is very similar to (2). Another example is given in [4], [30, Equation 2.50–2.51], where the following formula has been proposed for the

flow with $H = h^- - H^-$

$$Q = v^- H(k_c + k_d) = 0.15 - 0.45 \frac{(v^-)^2}{2gH} +$$

$$\left(0.57 - 2 \left(\frac{(v^-)^2}{2gH} - 0.21 \right)^2 \exp \left(10 \left(\frac{(v^-)^2}{2gH} - 0.21 \right) \right) \right).$$

The case of no weir, i.e., $H^- \equiv 0$ and $H^+ > 0$, lead to the following studied formulas, e.g. [27], [30, Equation 2.38]

$$Q = v^- 0.715 h^-$$

or [26], [30, Equation 2.39–2.42]

$$Q = v^- H^+ \left(h^- / H^+ \right)^{1.275}.$$

We restrict our discussion to the still commonly used (2) to outline the ideas. Further note that additional empirical formulas for the arising wave in the outgoing pooled step are not needed in our approach, since these dynamics are fully covered by the shallow–water equation.

For coupling conditions in the case of wide canals we refer to [16].

2. **The Riemann problem for a single weir.** By Riemann Problem at the weir we define the problem (1), (3) with initial data

$$(h, v) = \begin{cases} (h_l, v_l) & \text{for } x < 0 \\ (h_r, v_r) & \text{for } x > 0. \end{cases} \tag{4}$$

Definition 2.1. A solution to the Riemann Problem (1), (3), (4) is a function $(h, v) : \mathbb{R}^+ \times \mathbb{R} \to \mathbb{R}^2$ such that $(t, x) \to (h, v)(t, x)$ is self-similar and coincides in $x > 0$ with the restriction of the Lax solution to the standard Riemann Problem for (1) with initial data

$$(h, v) = \begin{cases} (h, v)(t, 0+) & \text{for } x < 0 \\ (h_r, v_r) & \text{for } x > 0. \end{cases} \tag{5}$$

while coincides in $x < 0$ with the restriction to of the Lax solution to the standard Riemann Problem for (1) with initial data

$$(h, v) = \begin{cases} (h_l, v_l) & \text{for } x < 0 \\ (h, v)(t, 0-) & \text{for } x > 0. \end{cases} \tag{6}$$

moreover $(h, v)(t, 0\pm) = (h^\pm, v^\pm)$ satisfy (3).

Remark that, being (h, v) self similar, $(h, v)(t, 0\pm)$ is constant.

For studying the Riemann problem we first collect the standard expressions for the eigenvalues, eigenvectors and Lax curves for the shallow water equations (1).

The 2×2 system of conservation laws in (1) has the eigenvalues λ_1, λ_2 and the eigenvectors r_1, r_2, where

$$\lambda_1(h, v) = v - \sqrt{gh} \qquad\qquad \lambda_2(h, v) = v + \sqrt{gh}$$

$$r_1(h, v) = \begin{bmatrix} -1 \\ -v + \sqrt{gh} \end{bmatrix} \qquad r_2(h, v) = \begin{bmatrix} 1 \\ v + \sqrt{gh} \end{bmatrix} \tag{7}$$

$$\nabla_{(h, hv)} \lambda_1(h, v) \cdot r_1(h, v) = \frac{3}{2} \sqrt{\frac{g}{h}} > 0 \quad \nabla_{(h, hv)} \lambda_2(h, v) \cdot r_2(h, v) = \frac{3}{2} \sqrt{\frac{g}{h}} > 0.$$

The Lax curves of the first and second family, described in Figure 2, are:

$$v = \mathcal{L}_1^+(h; h_0, v_0) = \begin{cases} v_0 - 2\left(\sqrt{gh} - \sqrt{gh_0}\right) & h \le h_0 \\ v_0 - (h - h_0)\sqrt{\frac{1}{2}g\frac{h+h_0}{hh_0}} & h > h_0, \end{cases} \tag{8}$$

$$v = \mathcal{L}_2^+(h; h_0, v_0) = \begin{cases} v_0 + 2\left(\sqrt{gh} - \sqrt{gh_0}\right) & h \ge h_0 \\ v_0 + (h - h_0)\sqrt{\frac{1}{2}g\frac{h+h_0}{hh_0}} & h < h_0. \end{cases} \tag{9}$$

The reversed Lax curves of the first and second family are given by:

$$v = \mathcal{L}_1^-(h; h_0, v_0) = \begin{cases} v_0 - 2\left(\sqrt{gh} - \sqrt{gh_0}\right) & h \ge h_0 \\ v_0 - (h - h_0)\sqrt{\frac{1}{2}g\frac{h+h_0}{hh_0}} & h < h_0, \end{cases} \tag{10}$$

$$v = \mathcal{L}_2^-(h; h_0, v_0) = \begin{cases} v_0 + 2\left(\sqrt{gh} - \sqrt{gh_0}\right) & h \le h_0 \\ v_0 + (h - h_0)\sqrt{\frac{1}{2}g\frac{h+h_0}{hh_0}} & h > h_0. \end{cases} \tag{11}$$

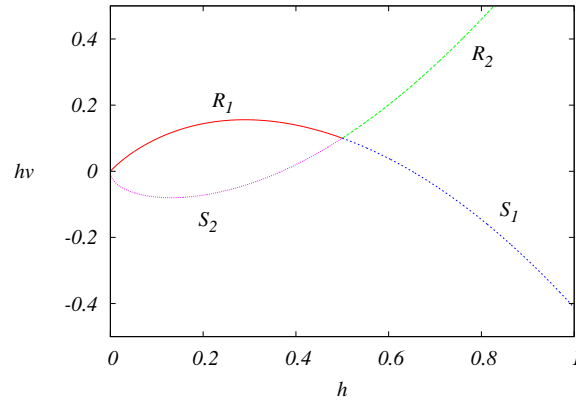Concerning the coupling condition, we study the states which satisfy it at the point

FIGURE 2. Lax curves for the shallow water system in the (h, hv) plane

$x = 0$. From (3), since the heights are always positive, it follows

$$\operatorname{sign} v^- = \operatorname{sign}\left(\left[h^- - H^-\right]_+ - \left[h^+ - H^+\right]_+\right).$$

Moreover

$$h^- \left|v^-\right| = C \left|\left[h^- - H^-\right]_+ - \left[h^+ - H^+\right]_+\right|^{\frac{3}{2}}$$

which becomes

$$\left(\frac{h^- \left|v^-\right|}{C}\right)^{\frac{2}{3}} = \left(\left[h^- - H^-\right]_+ - \left[h^+ - H^+\right]_+\right) \cdot \operatorname{sign} v^-,$$

$$\left[h^+ - H^+\right]_+ = \left[h^- - H^-\right]_+ - \left(\frac{h^- \left|v^-\right|}{C}\right)^{\frac{2}{3}} \cdot \operatorname{sign} v^-.$$

We have also to add the equality of the fluxes, hence we obtain

$$
\begin{cases}
[h^+ - H^+]_+ = [h^- - H^-]_+ - \left(\dfrac{h^- |v^-|}{C}\right)^{\frac{2}{3}} \cdot \operatorname{sign} v^- \\
h^+ v^+ = h^- v^-.
\end{cases}
\tag{12}
$$

Consider first the case where the water level to the right is below the weir, $h^+ \leq H^+$ so that $[h^+ - H^+]_+ = 0$. If also $h^- \leq H^-$ then no water crosses the weir, while if $h^- > H^-$ the water crosses the weir flowing from left to right. The left state must satisfy $v^- > 0$ and

$$
[h^- - H^-]_+ - \left(\frac{h^- |v^-|}{C}\right)^{\frac{2}{3}} = 0,
$$

which can be rewritten as

$$
h^- v^- = C [h^- - H^-]_+^{\frac{3}{2}}.
\tag{13}
$$

The curve (h^-, v^-) where h^-, v^- satisfy (13) consists of all the left states which can be connected to a right state with $h^+ \leq H^+$ (see Figure 3). The support of this curve lies in the upper part of the (h, hv) plane, hence we call it Γ_u. The case $h^+ \geq H^+$, $h^- < H^-$ is symmetric, hence we call Γ_l the support of the curve given by

$$
-h^+ v^+ = C [h^+ - H^+]_+^{\frac{3}{2}}.
$$

Since $C [h^- - H^-]_+^{\frac{3}{2}} = \tilde{C}\sqrt{g} [h^- - H^-]_+^{\frac{3}{2}} \leq \sqrt{g} (h^-)^{\frac{3}{2}}$, see (2), both Γ_u and Γ_l lie in the subcritical region. If both levels are above the weir, then (12) gives a unique state (h^+, v^+) which connects a given state (h^-, v^-) as we will see in the following Lemma.

Lemma 2.2. *Consider the (h, hv) plane, and define the following sets depicted in Figure 3:*

$$
\Omega_u = \left\{ (h, hv) : hv > C [h - H^-]_+^{\frac{3}{2}} \right\},
$$
$$
\Sigma_l = \left\{ (h, hv) : v < 0, \ 0 < h \leq H^- \right\},
$$
$$
A^- = \left\{ (h, hv) : 0 < hv < C [h - H^-]_+^{\frac{3}{2}} \right\},
$$
$$
B^- = \left\{ (h, hv) : v \leq 0, \ h > H^- \right\},
$$
$$
\Omega_l = \left\{ (h, hv) : hv < -C [h - H^+]_+^{\frac{3}{2}} \right\},
$$
$$
\Sigma_u = \left\{ (h, hv) : v > 0, \ 0 < h \leq H^+ \right\},
$$
$$
A^+ = \left\{ (h, hv) : v > 0, \ h > H^+ \right\},
$$
$$
B^+ = \left\{ (h, hv) : -C [h - H^+]_+^{\frac{3}{2}} < hv \leq 0 \right\}.
$$

Then, we have that the coupling condition induces the following assertions:

- *no left state $(h^-, h^- v^-) \in \Omega_u$ can be connected to any right state $(h^+, h^+ v^+)$ and no right state $(h^+, h^+ v^+) \in \Omega_l$ can be connected to any left state $(h^-, h^- v^-)$;*
- *any left state in Γ_u can be connected to any right state in Σ_u with the same flux: $h^- v^- = h^+ v^+$;*
- *any right state in Γ_l can be connected to any left state in Σ_l with the same flux: $h^- v^- = h^+ v^+$;*

- *any left state in A^- can be connected to one and only one right state in A^+ and any right state in A^+ can be connected to one and only one left state in A^-;*
- *any left state in B^- can be connected to one and only one right state in B^+ and any right state in B^+ can be connected to one and only one left state in B^-.*
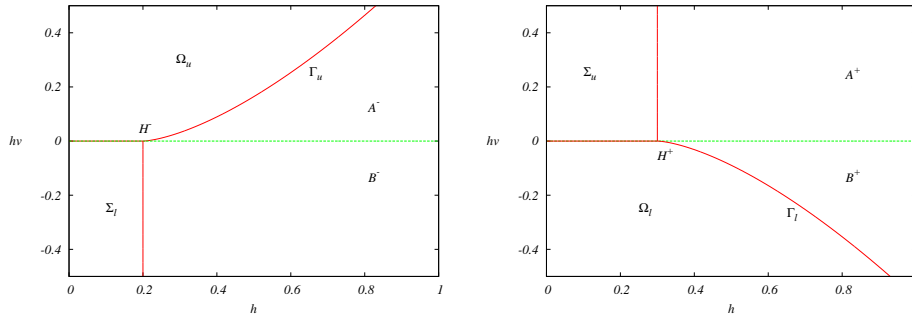

FIGURE 3. Representation of the regions introduced in Lemma 2.2

We omit the proof since it is a straightforward analysis of the coupling conditions (12).

We call $\Phi : A^- \cup B^- \to A^+ \cup B^+$ the one to one map that associates to any left state in $A^- \cup B^-$ the corresponding right state in $A^+ \cup B^+$ connected through the coupling condition:

$$\Phi(h, hv) = \left(H^+ + h - H^- - \left(\frac{h|v|}{C} \right)^{\frac{2}{3}} \operatorname{sign} v, hv \right).$$

We also define

$$\Phi(h, hv) = \left((-vh/C)^{\frac{2}{3}} + H^+, hv \right) \in \Gamma_l, \quad \text{for any } (h, hv) \in \Sigma_l,$$

in such a way that the right state $(h^+, h^+ v^+) = \Phi(h^-, h^- v^-)$ is connected through the coupling condition to the left state $(h^-, h^- v^-)$ for any $(h^-, h^- v^-) \in \Sigma_l \cup A^- \cup B^-$.

We are now able to show that the Riemann problem can be solved in the large.

Proposition 1. *For all states (h_l, v_l) and (h_r, v_r) in the subcritical region, the Riemann problem (1), (3), (4) has a unique solution satisfying Definition 2.1, whose constant states depend continuously on the initial data and are constructed gluing together a wave of the first family, the coupling condition and a wave of the second family.*

Proof. Given two states (h_l, v_l) and (h_r, v_r) in the subcritical region, we proceed in the following way for solving the Riemann problem. Draw the Lax curve of the first family in the (h, hv) plane through (h_l, v_l). Since, in the subcritical region, the function whose graph is the support of this Lax curve is strictly decreasing, it intersects in one and only one point (with $h > 0$) Γ_u since it is the graph of

a convex and non decreasing function. We call the unique point of intersection (h^*, v^*). Then, we consider the curve

$$\gamma(h) = \begin{cases} \left(\frac{H^+}{h^*} h, h^* v^* \right) & \text{for } h \leq h^* \\ \Phi \left(h, h \mathcal{L}_1^+ (h; h_l, v_l) \right) & \text{for } h > h^*. \end{cases} \tag{14}$$

It can be checked that its support is the graph of a non increasing function. Next, we take the inverse Lax curve related to the second characteristic field passing through the right state (h_r, v_r). The support of this curve, in the subcritical region and in the upper supercritical region is the graph of a strictly increasing function, therefore it has one and only one point of intersection with γ (for positive h), denoted by (k, w). This point might belong to the upper supercritical region. The Riemann problem is finally solved in the following way: take the subcritical (or lower supercritical) state (k^*, w^*) on the first Lax curve such that $kw = k^* w^*$ and connect (h_l, v_l) to (k^*, w^*) with a wave of the first family. This wave has negative velocity since the curve belongs entirely to the subcritical region or to the subcritical region and the lower supercritical one. Then, the points (k^*, w^*) and (k, w) satisfy the coupling conditions (3). Finally (k, w) and (h_r, v_r) are connected by a wave of the second family which travels with positive velocity even if (k, w) happens to be in the upper supercritical region, see Figure 4. □
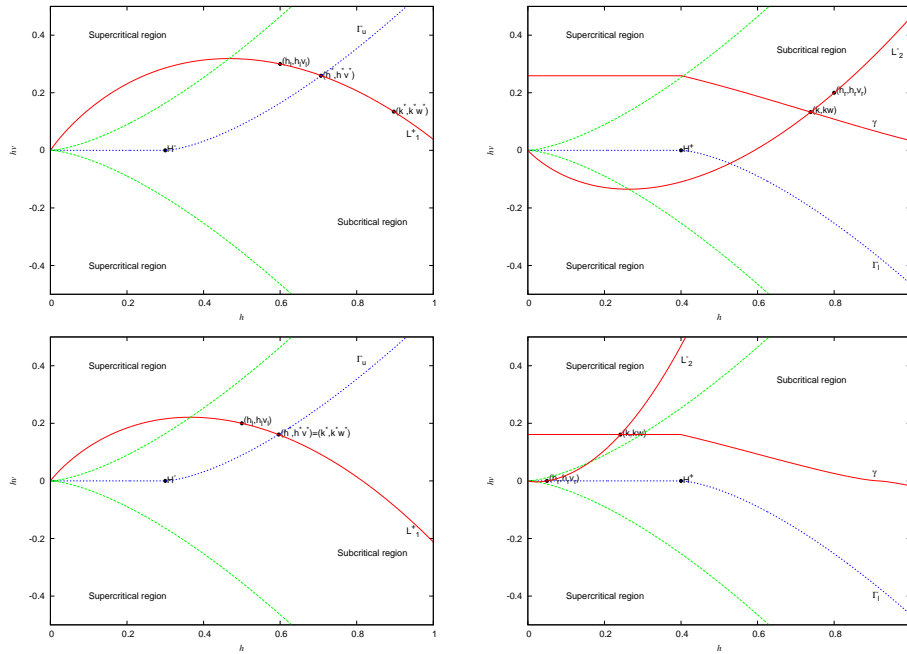

FIGURE 4. These figures describe how to solve two Riemann Problem (first and second row). The states on the left and on the right of the weir are represented respectively on the left and right figures. The green lines separate the subcritical and supercritical regions

3. **A well posedness result.** This section is devoted to show the well–posedness of the Cauchy problem for system (1) for initial data around a constant subcritical state satisfying the coupling condition (3). For simplicity we suppose that the water level to the right of the weir is below the weir level, that is $h^+ < H^+$. This implies that the water can only flow from the left to the right of the weir when its left level overflows the weir.

Theorem 3.1. *Given H_0^-, H^+ and two constant states in the subcritical region (h_0, v_0) and (h_1, v_1) such that*

$$h_0 v_0 = C\left[h_0 - H_0^-\right]_+^{\frac{3}{2}}, \quad h_0 v_0 = h_1 v_1, \quad h_0 > H_0^-, \quad h_1 < H^+, \qquad (15)$$

then, there exists a closed domain

$$\mathcal{D} \subseteq \left\{(h, v) \in (h_0, v_0)\chi_{(-\infty,0)} + (h_1, v_1)\chi_{(0,\infty)} + (Ł1 \cap \mathbf{BV})\left(\mathbb{R}; \mathbb{R}^2\right)\right\}$$

containing all functions with sufficiently small total variation in $x > 0$ and $x < 0$ and semigroups

$$S_t^{H^-} : \mathcal{D} \to \mathcal{D}$$

defined for all H^- sufficiently close to H_0^-, such that
1) for all $t, s \geq 0$ and $u \in \mathcal{D}$

$$S_0^{H^-} u = u, \qquad S_t^{H^-} S_s^{H^-} u = S_{t+s}^{H^-} u;$$

2) for all $u, v \in \mathcal{D}$, H_1^-, H_2^- in a suitable neighborhood of H_0^- and $t, t' \geq 0$:

$$\left\| S_t^{H_1^-} u - S_{t'}^{H_2^-} v \right\|_{Ł1} \leq L \cdot \left\{ \|u - v\|_{Ł1} + |t - t'| + t \cdot |H_1^- - H_2^-| \right\};$$

3) if $u \in \mathcal{D}$ is piecewise constant, then for t small, $S_t^{H^-} u$ is the glueing of solutions to Riemann problems at the points of jump in u and at the weir in $x = 0$;
4) for all $u_o \in \mathcal{D}$, the map $u(t, x) = \left(S_t^{H^-} u_o\right)(x)$ is a weak entropy solution to (1), (3) (see [6, Definition 4.1], [12, Definition 2.1]).
S is uniquely characterized by 1), 2) and 3).

Proof. Following [13, Proposition 4.2], the 2×2 system (1) defined for $x \in \mathbb{R}$ can be rewritten as the following 4×4 system defined for $x \in \mathbb{R}^+$:

$$\begin{cases} \partial_t U + \mathcal{F}(U) = 0 & (t, x) \in \mathbb{R}^+ \times \mathbb{R}^+ \\ b\left(U(t, 0+)\right) = g(t) & t \in \mathbb{R}^+. \end{cases} \qquad (16)$$

the relation between U and $u = (h, v)$, between $\mathcal{F}$ and the flow in (1) being:

$$U(t, x) = \begin{bmatrix} h(t, -x) \\ -(hv)(t, -x) \\ h(t, x) \\ (hv)(t, x) \end{bmatrix} \qquad \mathcal{F}(t, x) = \begin{bmatrix} U_2 \\ \frac{U_2^2}{U_1} + \frac{1}{2}gU_1^2 \\ U_4 \\ \frac{U_4^2}{U_3} + \frac{1}{2}gU_3^2 \end{bmatrix} \qquad (17)$$

with $x \in \mathbb{R}^+$; whereas the boundary conditions becomes

$$g(t) \doteq \begin{pmatrix} H^- - H_0^- \\ 0 \end{pmatrix}, \quad b(U) \doteq \begin{pmatrix} U_1 - \left(-\frac{U_2}{C}\right)^{\frac{2}{3}} - H_0^- \\ U_4 + U_2 \end{pmatrix}.$$

The thesis now follows from [12, Theorem 2.2]. Indeed the assumptions (γ), $(\mathbf{b})$ and $(\mathbf{f})$ are therein satisfied. More precisely the eigenvalues of the Jacobian of the flow in (17) are

$$\frac{U_2}{U_1} \pm \sqrt{gU_1}, \qquad \frac{U_4}{U_3} \pm \sqrt{gU_3};$$

therefore in the subcritical region exactly two are positive and exactly two are negative. Since here $\gamma(t) = 0$, $\dot\gamma(t) = 0$, condition (γ) in [12, Theorem 2.2] is satisfied with $\ell = 2$. Concerning condition $(\mathbf{b})$, the positive eigenvalues with the corresponding eigenvectors evaluated at $\overline{U} = (h_0, -h_0 v_0, h_1, h_1 v_1)$ are

$$\Lambda_3 = -v_0 + \sqrt{gh_0}, \quad R_3 = \begin{pmatrix} 1 \\ -v_0 + \sqrt{gh_0} \\ 0 \\ 0 \end{pmatrix}$$

$$\Lambda_4 = v_1 + \sqrt{gh_1}, \quad R_4 = \begin{pmatrix} 0 \\ 0 \\ 1 \\ v_1 + \sqrt{gh_1} \end{pmatrix}.$$

Conditions (15) imply $b\left(\overline{U}\right) = 0$, and

$$\left[Db(\overline{U})R_3, \; Db(\overline{U})R_4\right] = \begin{bmatrix} 1 + \frac{2}{3C}\left(\sqrt{gh_0} - v_0\right) \cdot \left(-\frac{U_2}{C}\right)^{-\frac{1}{3}} & 0 \\ -v_0 + \sqrt{gh_0} & v_1 + \sqrt{gh_1} \end{bmatrix}.$$

The determinant of the above matrix is given by

$$\left(1 + \frac{2}{3C}\left(\sqrt{gh_0} - v_0\right) \cdot \left(-\frac{U_2}{C}\right)^{-\frac{1}{3}}\right)\left(v_1 + \sqrt{gh_1}\right)$$

which is strictly positive since (h_0, v_0) and (h_1, v_1) belong to the subcritical region. Thus condition $(\mathbf{b})$ is satisfied. Concerning condition $(\mathbf{f})$, system (16) is not necessarily strictly hyperbolic, for it is obtained glueing two copies of system (1). Nevertheless, the two systems are coupled only through the boundary conditions, hence the whole wave front tracking procedure in the proof of [12, Theorem 2.2] applies. Concerning the Lipschitz dependence on the height H^-, observe that as in [12, Theorem 2.2] we have for

$$g(t) = \begin{pmatrix} H_1^- - H_0^- \\ 0 \end{pmatrix}, \qquad \bar{g}(t) = \begin{pmatrix} H_2^- - H_0^- \\ 0 \end{pmatrix},$$

and hence

$$\int_0^t |g(\tau) - \bar{g}(\tau)| \, d\tau = \int_0^t \sqrt{\left[\left(H_1^- - H_0^-\right) - \left(H_2^- - H_0^-\right)\right]^2 + 0^2} \, d\tau$$
$$= t \cdot \left|H_1^- - H_2^-\right|.$$

$\square$

4. **Computational results.** We present some numerical results on pooled steps using a finite–volume method in the conservative variables to solve for the system dynamics in each canal. The coupling conditions (3) induce boundary conditions for each canal at each time–step. For given data $U_0^\pm := (h_0^\pm, (hv)_0^\pm)$ close to the weir the conditions yield the boundary states at each connected canal. In the numerical computation of the boundary states we proceed as in Section 2 using Newton's

method applied to (3) where $h^\pm$ and $(hv)^\pm$ are given by the forward (backwards) 1-(2) Lax–wave curves through the initial state $h_0^\pm, (hv)_0^\pm$.

According to the solution of the Riemann Problem described in Section 2 there are three possible scenarios. If $h^\pm \leq H^\pm$ the coupling condition (3) reduce to $v^\pm = 0$ and no water passes the weir. If $h^- > H^-$ and $h^+ \leq H^+$ the water is overflowing the weir from the left to the right. If $h^+ > H^+$ and $h^- \leq H^-$ the water is overflowing the weir from the right to the left. If $h^+ > H^+$ and $h^- > H^-$ the water is flowing from the left or from the right depending on the sign of $(h^- - H^-) - (h^+ - H^+)$.

Now, we present a numerical result for overflowing three connected pooled–steps. Each canal has length $L = 1$ and the height of each weir is 1.5. We simulate two situations using a Lax–Friedrich finite volume scheme on a uniform grid with spacing $N_x = 100$ per canal. The time–step is such that the CFL conditions holds. In the first case the initial water level in each canal is low (equal to H^-) (see Figure 5) and in the second case the canals are already full (height is equal to H^+) (see Figure 6). In both cases the water initial is still $v = 0$ and a wave with a height $h = 2\,H^+$ and $hv = 5$ enters on the first canal. This wave lasts until $T = 20$ and is then followed by a wave of height $h = H^-$ and zero flux. The simulation time is $T = 60$ for both scenarios. We present snapshots of height and velocity at different times. The solid lines are the weir, the dotted line is ground level. It is a pooled step and therefore the first canal is on a higher level above ground than the last one.

In the first scenario (see Figure 5) the wave enters the system of pooled steps and overflows the connected canals. After this wave passed the system slowly reaches again an almost steady state. In the second scenario (see Figure 6) we observe initial dynamics due to the overflow of the pooled steps. On the second canal these dynamics interact with the incoming wave. After the wave passed the system slowly reaches a steady state with heights below critical (i.e., $h \leq H^+$) in the first and second canal. The water is still flowing over the third weir in this simulation.
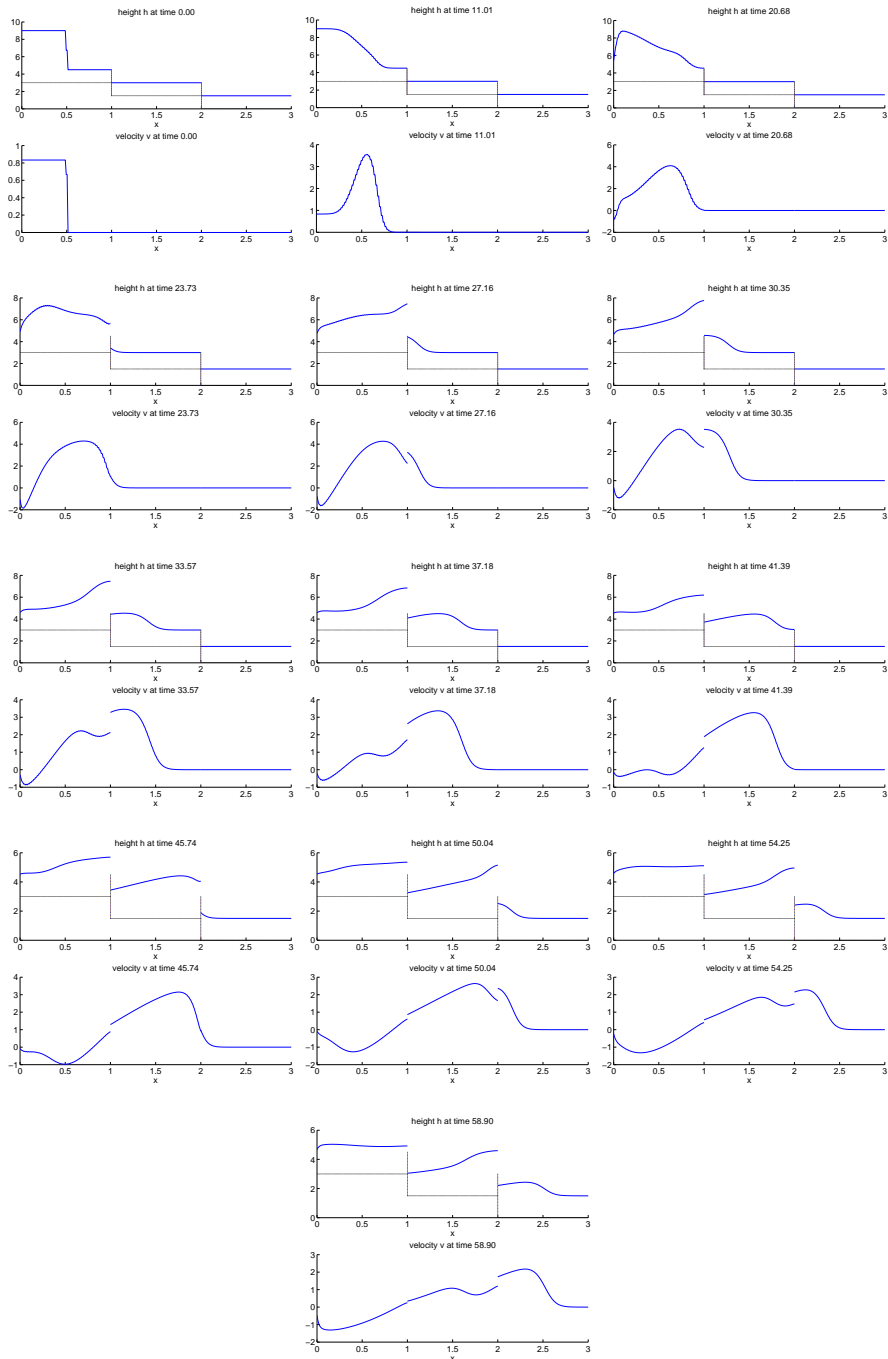
FIGURE 5.   Simulation results for a strong wave entering the pooled step. Initially, the water level on each step is below critical. The solution (h, v) at different times is depicted. The time increases from left to right and top to bottom.
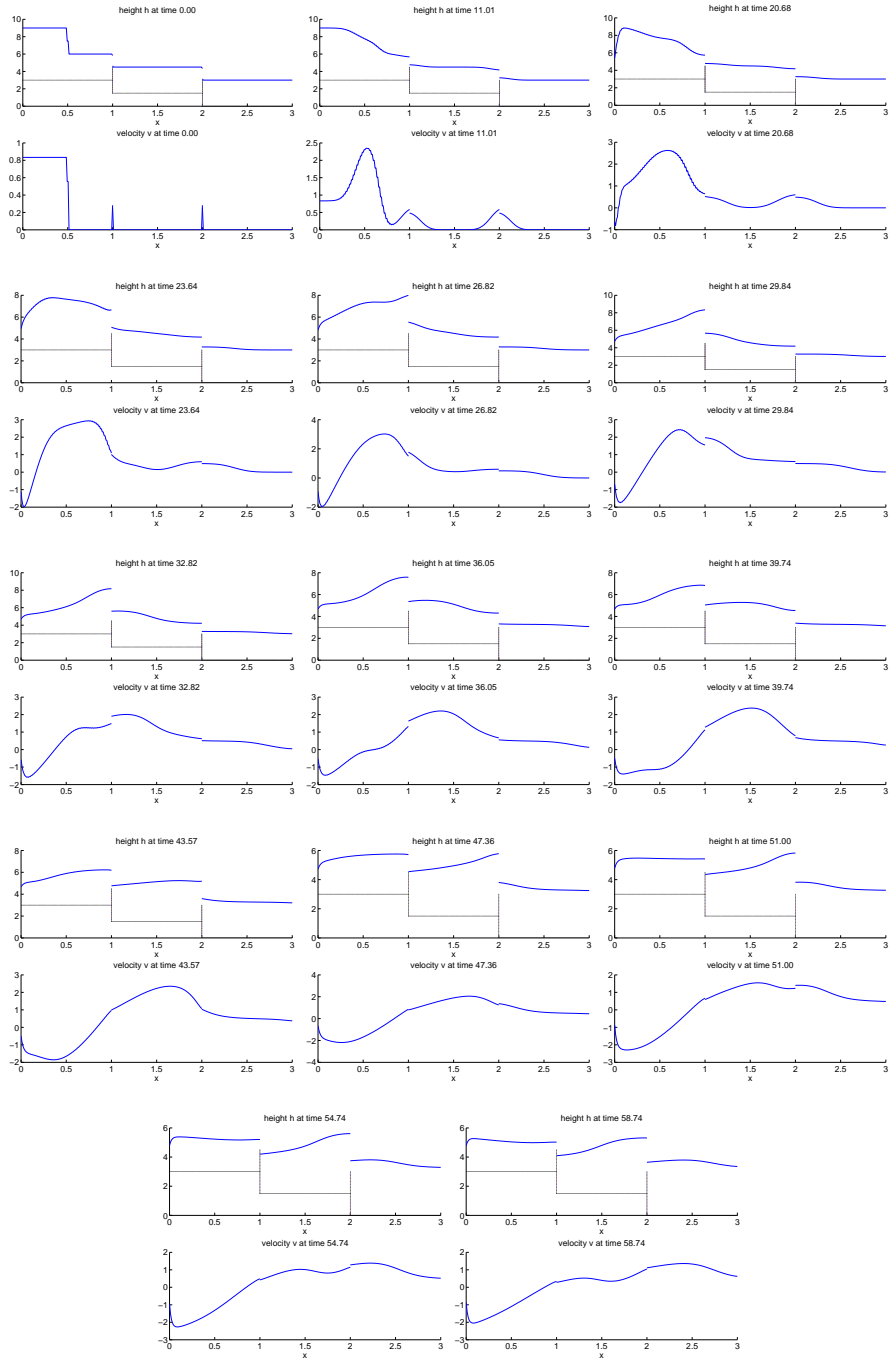
FIGURE 6.   Simulation results for a strong wave entering the
pooled step. Initially, the water level on each step is above the
critical level. The solution (h, v) at different times is depicted.
The time increases from left to right and top to bottom.

REFERENCES

[1] M. K. Banda, M. Herty and A. Klar, *Coupling conditions for gas networks governed by the isothermal Euler equations*, Networks and Heterogeneous Media, **1** (2006), 295–314.

[2] M. K. Banda, M. Herty and A. Klar, *Gas flow in pipeline networks*, Networks and Heterogeneous Media, **1** (2006), 41–56.

[3] G. Bastin, B. Haut, J.-M. Coron and B. D'Andréa-Novel, *Lyapunov stability analysis of networks of scalar conservation laws*, Netw. Heterog. Media, **2** (2007), 751–759 (electronic).

[4] F. W. Blaisdell, *Equation for the free-falling nappe*, Proceedings ASCE, no. 482, **80** (1954).

[5] J. N. Bradley and A. J. Peterka, *The hydraulic design of sitlling basins*, Journal of the Hydraulics Division, **83** (1957) 1401.1–1401.24.

[6] A. Bressan, "Hyperbolic Systems of Conservation Laws. The One-Dimensional Cauchy Problem," Oxford Lecture Series in Mathematics and its Applications, **20**, Oxford University Press, Oxford, 2000.

[7] M. Chamani and N. Rajaratnam, *Jet flow on stepped spillways*, Journal of the Hydraulic Engineering, **125** (1994), 254–259.

[8] H. Chanson, *Comparison of energy dissipation between nappe and skimming flow regimes on stepped chutes*, Journal of the Hydraulic Research, **32** (1994), 213–218.

[9] H. Chanson, "Hydraulic Design of Stepped Cascades, Channels, Weirs and Spillways," Pergamon Press, Oxford, England, 1994.

[10] H. Chanson, "The Hydraulics of Stepped Chutes and Spillways," Taylor & Francis, 2002.

[11] R. M. Colombo and M. Garavello, *On the Cauchy problem for the p-system at a junction*, SIAM J. on Math. Anal., **39** (2008), 1456–1471.

[12] R. M. Colombo and G. Guerra, *On general balance laws with boundary*, J. Differential Equations, **248** (2010), 1017–1043.

[13] R. M. Colombo, G. Guerra, M. Herty and V. Schleper, *Optimal control in networks of pipes and canals*, SIAM J. Control Optim., **48** (2009), 2032–2050.

[14] R. M. Colombo and F. Marcellini, *Smooth and discontinuous junctions in the p-system*, J. Math. Anal. Appl., **361** (2010), 440–456.

[15] R. M. Colombo and C. Mauri, *Euler system for compressible fluids at a junction*, Journal of Hyperbolic Differential Equations, **5** (2008), 547–568.

[16] J. de Halleux, C. Prieur, J.-M. Coron, B. d'Andréa Novel and G. Bastin, *Boundary feedback control in networks of open channels*, Automatica J. IFAC, **39** (2003), 1365–1376.

[17] V. Dos Santos, G. Bastin, J.-M. Coron and B. d'Andréa Novel, *Boundary control with integral action for hyperbolic systems of conservation laws: Stability and experiments*, Automatica J. IFAC, **44** (2008), 1310–1318.

[18] R. Dressler, *Mathematical solution to the problem of roll-waves in inclined open channels*, Communication in Pure and Applied Mathematics, **2** (1949), 149–194.

[19] M. El-Kmamash, M. Loewen and N. Rajarantnam, *An experimental investigation of jet flow on a stepped chute*, Journal of Hydraulic Research, **43** (2005), 31–43.

[20] G. Guerra, F. Marcellini and V. Schleper, *Balance laws with integrable unbounded sources*, SIAM J. Math. Anal., **41** (2009), 1164–1189.

[21] M. Gugat, *Nodal control of conservation laws on networks*, in "Control and Boundary Analysis" (eds. John Cagnol, et al.), Lecture Notes in Pure and Applied Mathematics, **240**, Chapman & Hall/CRC, Boca Raton, FL, (2005), 201–215.

[22] G. Leugering and E. J. P. G. Schmidt, *On the modelling and stabilization of flows in networks of open canals*, SIAM J. Control Optim., **41** (2002), 164–180 (electronic).

[23] X. Litrico, V. Fromion, J.-P. Baume, C. Arranja and M. Rijo, *Experimental validation of a methodology to control irrigation canals based on saint-venant equations*, Control Engineering Practice, **13** (2005), 1425–1437.

[24] A. Marigo, *Entropic solutions for irrigation networks*, SIAM J. Appl. Math., **70** (2009/10), 1711–1735.

[25] I. Ohtsu, Y. Yashuda and M. Takahashi, *Flow characteristics of skimming flows in stepped channels*, Journal of Hydraulic Engineering, **130** (2004), 860–869.

[26] W. Rand, *Flow geometry at straight drop spillways*, Proceedings ASCE, no. 791, **81** (1955).

[27] H. Rouse, *Discharge characteristics of the free overfall*, Civil Engineering, **6** (1936), 257–260.

[28] R. M. Sorenson, *Stepped spillway hydraulic model investigation*, Journal of Hydraulic Engineering, **111** (1985), 1461–1472.

[29] T. Sturm, "Open Channel Hydraulics," McGraw-Hill, 2001.

[30] J. Thorwarth, "Hydraulisches Verhalten von Treppengerinnen mit eingetieften Stufen - selbstinduzierte Abflussinstationariäten und Energiedissipation," Ph.D Thesis, RWTH Aachen University, Department of Civil Engineering. 2008.

Received October 2010; revised August 2011.

E-mail address: graziano.guerra@unimib.it
E-mail address: herty@mathc.rwth-aachen.de
E-mail address: f.marcellini@campus.unimib.it